Performance of the trigger hodoscopes in 2007 and 2010

K. Novotny[a], E.-M. Kabuss[b]

[a] *PRISMA Cluster of Excellence & Institut für Physik (THEP) Johannes Gutenberg-Universität, D55099 Mainz, Germany*
[b] *Institute of nuclear physics, Becherweg 45, D55099 Mainz, Germany*

The Note gives an overiew of a study of the performance of the triggerhodoscopes between 2007 and 2010. Furthermore it shows an estimate of the efficiencies of the hodoscopes. Also observations concerning the distribution of tracks at the different hodoscope planes are summarised.

Contents

1 The muon trigger system

For the data taking with the muon beam a trigger system is set up that relies on the detection of scattered muons and on energy deposit in one of the hadron calorimeters. The muons are detected behind thick concrete or iron absorbers for muon identification either by measuring their scattering angle, so called target pointing trigger, or measuring the energy loss using the deflection in the dipoles, the so-called energy loss trigger. Target pointing relies on the measurement of the scattering angle in a direction perpendicular to the bending through the dipoles, thus requires horizontal scintillator strips in COMPASS. The width of the strips is given by multiple scattering in the target, the length of the target material along the beam line and the distance to the muon beam. On the other hand the energy loss trigger has vertical strips with a width determined by the distance to the dipole and the required momentum resolution[1, 2]. The muon trigger system is operated since 2003. Figure 1 shows the COMPASS spectrometer setup of 2010:

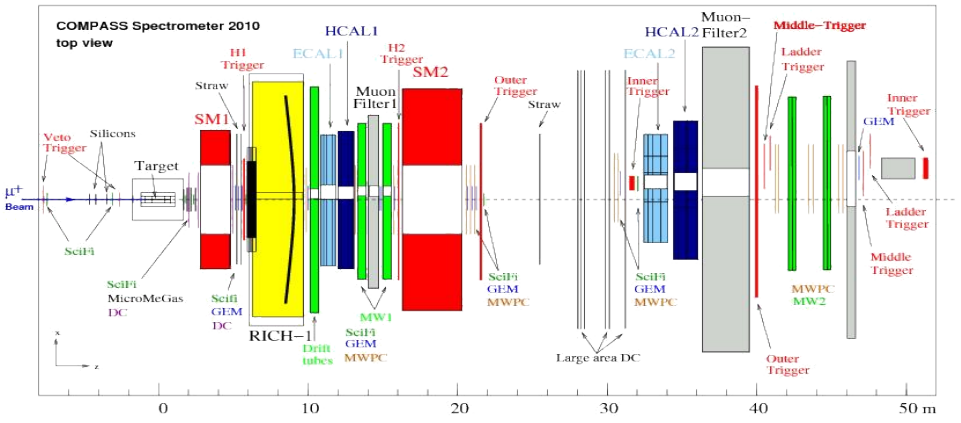

Figure 1: COMPASS spectrometer setup of 2010[1]

The measurements used the existing hodoscope system selecting inclusive events, which is operated since 2002 at the COMPASS experiment and which was continuously improved during the recent years. The actual hodoscope system is shown in figure 2. Due to the large variation of counting rates, different trigger systems are being used for different kinematic regions. These parts are discussed in the following subsection[1, 2].

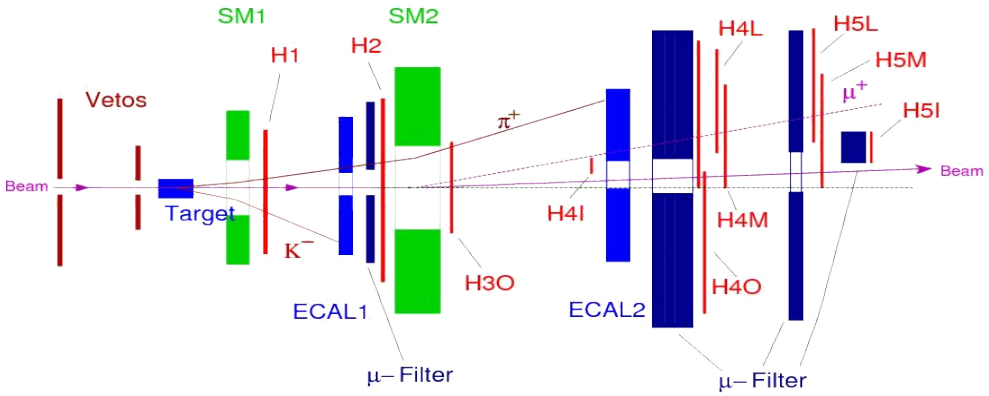

Figure 2: Location of the components relevant for the trigger [1]

1.1 The trigger hodoscopes

In order to guarantee triggering on muons only, at least one of the two hodoscopes is located behind an absorber (muon filter). In each case, the hodoscopes are put as close as possible to the absorber to minimize effects due to multiple Coulomb scattering in the absorber [1, 2].

The inner trigger: The inner trigger measures the energy loss of scattered muons in the range of small energy losses y using H4I and H5I with vertical hodoscope elements. A fine granularity is used to achieve a good minimum y cut $y_{min} \approx 0.2$ and to cope with the high rates close to the beam. For this reason each of the hodoscopes is also split into an upper and a lower part. The elements are read out by PMTs on one side. For muon identification an iron absorber in front of H5I is used (MF3).The inner trigger covers the region of $0.2<y<0.5$ with very small Q^2[3].

The ladder trigger: The ladder trigger selects muons with small scattering angles but high energy losses. To achieve this selection, the ladder hodoscopes are located behind the spectrometer magnets bending particles in the horizontal plane. The ladder hodoscopes consist of short vertical strips read out on both sides by PMTs. Using a coincidence of two hodoscope strips in H4L and H5L, muons with a large deflection in

the magnets but very small scattering angle are selected yielding events with a large energy loss, but small Q^2[1, 2].

The middle trigger: The middle trigger combines the features of an energy loss trigger using vertical elements with a target pointing trigger using a second layer of horizontal strips for each of the two hodoscopes. The vertical strips are readout on one side by PMTs while the horizontal ones are read on both sides. The middle system covers a relative energy transfer y from 0.1 to 0.7 at small scattering angles from 5 mrad to 10 mrad[1, 2].

The outer trigger: The outer system consists of a horizontal hodoscope plane at the exit of the second spectrometer magnet (H3O) and a second one behind the hadron absorber in the SAS (H4O) to obtain vertical target pointing. It is divided into two halves to avoid very long strips. The size of the second hodoscope is matched to the size of the muon wall MW2 chambers used to reconstruct muon tracks. All strips are read out by two PMTs. The outer system covers all y and large Q^2 up to 10 $\left(\frac{GeV}{c}\right)^2$[1, 2].

The LAS trigger: The LAS trigger system was set up for the 2010 transverse data taking. It consists of two horizontal hodoscope planes, H1 in front of the RICH and H2 after the first muon filter and the muon wall MW1 modules. The size of the second hodoscope is matched to the size of the MW1 chambers measuring the tracks behind the first muon filter. It is split into two halves to avoid too long strips and to allow an easy triggering on muon pairs in the future Drell-Yann programme. All scintillator elements are read out by two PMTs. Similar to the outer system the LAS system makes use of vertical target pointing. The main purpose of this system is the extension of the muon trigger system to the largest Q^2 and high x_B [1, 2].

1.2 Calorimeter trigger

Events containing muons with small scattering angles do not only stem from quasi-real photo production with large energy transfers, but also from a number of background processes with high rate e.g., radiative events. Requiring in addition a hadronic energy loss in one of the calorimeters can reduce these backgrounds considerably. But the calorimeters have to cope with a high rate of halo muons of 5 $\times 10^6$ per second passing through the calorimeter depositing an average energy of 1.8 GeV. Thus, it is not possible to trigger on the energy deposit in the whole calorimeter, but the energy deposit in 4×4 calorimeter cells is measured and a threshold above the energy deposit of a muon is used in the trigger [3]. The concept of this trigger method is shown in Fig. 3.

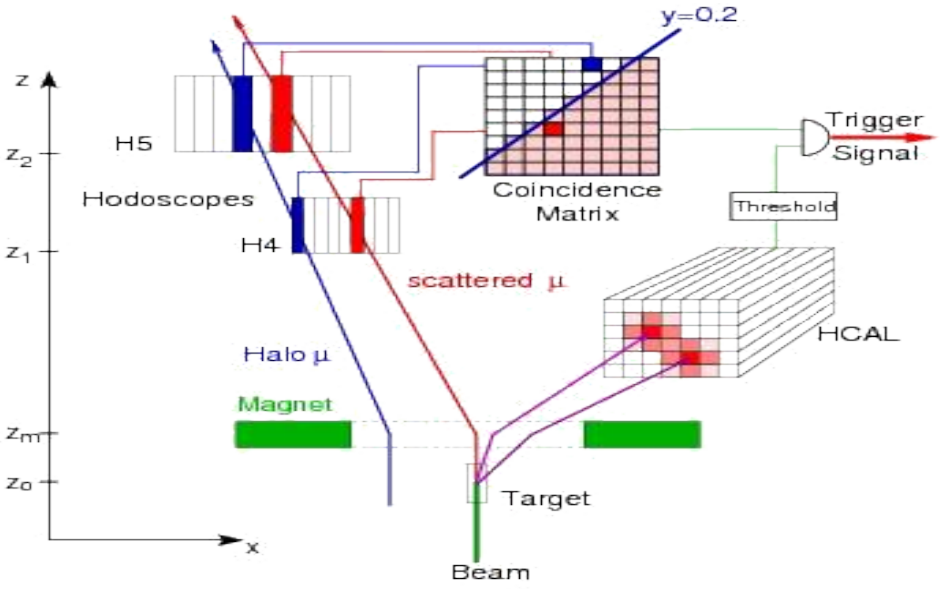

Figure 3: Concept of the trigger [3]

Such a calorimeter trigger is used in two different ways. In one trigger, the energy depost in one of the calorimeters is required in addition to a small angle trigger to reduce fake triggers due to halo muons or beam muons with large angles due to multiple scattering in the target. Secondly, a high threshold is used allowing to extend the trigger acceptances to regions not covered by hodoscopes. The pure calorimeter trigger is also used to determine the efficiency of the hodoscope planes.

2 Analysis method

2.1 Method

For the study of the trigger hodoscope performance the method developed by Konrad Klimaszewski for the analysis of the 2004 and 2006 muon data was used. The method relies on the pure calorimeter trigger where only energy deposits in the calorimeter are required [3].
Reconstructed events with a vertex and an identified scattered muon are selected. In the reconstruction of pure calorimeter events no hodoscope hits are required for the scattered muons, but if hits in a hodoscope are consistent with a track they will be attached to the track and the track fit eventually improved. This allows on PHAST level to study the performance of the hodoscopes and determine a efficieny along the strips for most hodoscope planes by counting the numbers of tracks passing a certain hodoscope strips and the tracks with a hit attached in this hodoscope. In spectrometer regions with low number of the tracking planes this method yields only an upper limits of the efficiency. Nevertheless the data can be used to study the time dependence of the hodoscope performance and the distribution of tracks ob the hodoscopes.
There is one exeception. For muons passing through the inner hodoscopes H4I and H5I muon identification relies on the muon filter MF3 in front of H5I. There is no other tracking detector behind MF3. So for muon identification a hit is required in H5I which makes it impossible to determine the efficiency. But the distribution of tracks across H5I still can be used to check for weak elements.
For all other hodoscope planes there are tracking detector behind the corresponding muon filter so that hodosope hits are not required for muon identification.

2.2 Data selection

The data selection is done on PHAST level using a UserEvent based on the one provided by Konrad Klimszewski[4]. The following selections and cuts are applied to the data:
The triggerbit of the calorimetric triggerbit is required. Muons are selected from the best primary vertex with more than one outgoing particle and must have more than 6 hits behind Muon Filter 2, a momentum larger than 40 GeV and they must have passed more than 30 radiation length. A beam σ_{time} of less than 10 ns is required. UserEvent31415 was made faster by a factor of 2. The best primary vertex was chosen immediately, contrary to Konrad Klinszweskis UserEvent, where a particle-check was executed at first. This check was removed and a cut on the CORAL PID 5 for μ^+ and on CORAL PID 6 for μ^- was introduced. This cut was also introduced in the loop over the outgoing particles to assure that the detected particles is muon.
In addition to the various target cuts, a variable target cut was introduced, which accesses the information on the mDSTs.
This UserEvent can also be used for 2004 and 2006 data.

2.3 Analysis of 2010 data

In principle the structure is the same as described in section 2.2. New in the 2010 data is the presence of the LAS trigger hodoscopes. At the time of this analysis the LAS trigger was not yet fully implemented in CORAL. The target cut was the same as in 2007, because at the time of evaluating the productions of 2010 the target cut alignment had not yet been finished.

3 Results

During evaluating the data, few unexpected observations were made when checking the distribution of tracks on the different hodoscopes.

3.1 Distribution of Tracks

As a first step the distribution of muons at the different hodoscopes and the distribution of muons with a hit in the hodoscope were investigated. For this purpose a fine histogram binning is used with 6 bins across each hodoscope strip. The analysis was done for two weeks from 2007 and one week of 2010. The results also were compared to results previously obtained by Konrad Klimaszewski for the 2004 and 2006 data. Figure 4 shows as an example the muon efficiencies in HO04 jura. In the region with scintillator material a uniform distribution of tracks is observed except for one weak element at the bottom. In 2010 the 4 central strips were exchanged with longer scintillators to cover the acceptance hole between the outer and the middle hodoscopes. The extension of all four central elements is clearly visible on the right plot. As a second example, the track distribution in HM05 is presented in Fig.5. Here, not only the muon distribution with hits in HM05 but also the distribution of extrapolations is shown for 2007. The special features are also seen in the data from other years. They are discussed in the next section.

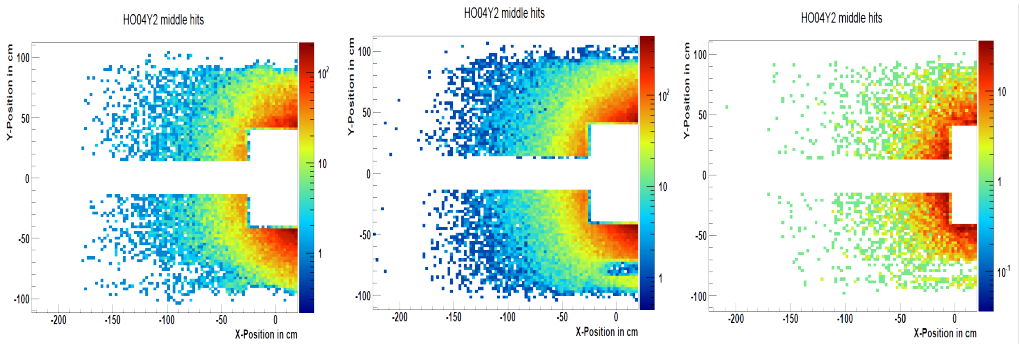

(a) 07W25 (b) 07W44 (c) 10W39

Figure 4: Distribution of tracks in the Hodosocope HO04

3.2 Special features

The structure seen in the distribution on Fig. 5 are also present in the 2004 and 2006 data. But as in these analyses only the central high efficiency parts were of interest, the observed structures were not discussed in detail by Konrad Klimaszewski.

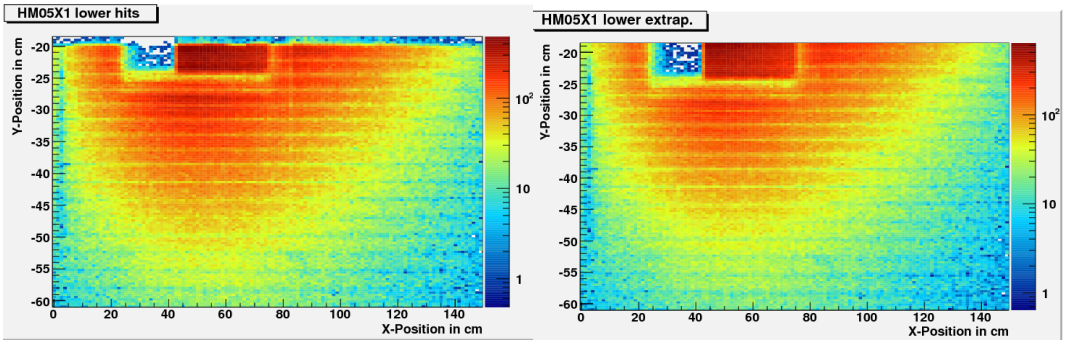

(a) Hits (b) Extrapolation

Figure 5: Distribution of tracks and extrapolation in the low part of HM05

The observations are:

1. Horizontal bands
2. Region without extrapolation
3. "Shadow" of chamber

1. The first effect stems from the inclusion of the hosdopscopes as tracking detectors in CORAL.In most cases the inclusion of hodoscope hits does not influence the track parameters a lot due to the moderate space resolution of the hodoscopes. Only for planes with high granularity in a region with only few other detectors measuring the same coordinate, hodoscope hits can have an impact on the track parameters. The former implementation in CORAL produces a non-uniform distribution of tracks across the strips. So only the efficiency along the strips but not across the strips can be determined.

2. On the upper part of the distributions in Fig.5 a rectangular region of about 15cm $\times$ 5cm with very few extrapolations and tracks is visible. To investigate this region more detailed a special study was done. Without any cuts due to hodoscope sensitive areas two distributions were obtained at Z=41m, roughly at the position of the first middle trigger hodoscope.

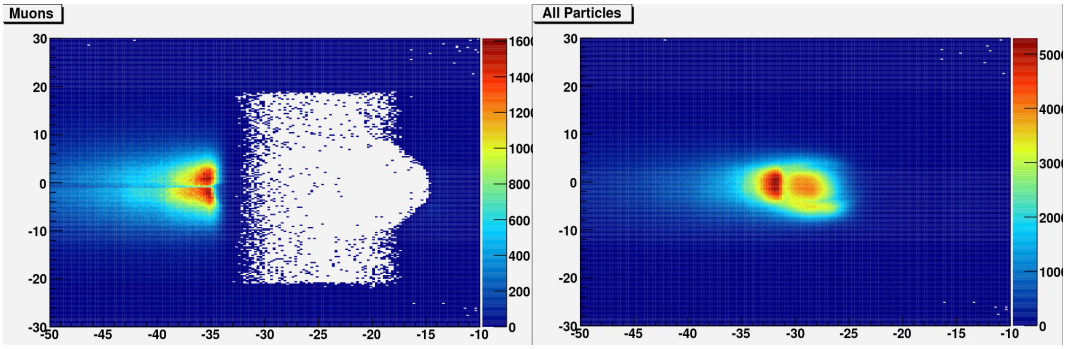

(a) Muons (b) All Particles

Figure 6: Distributions of muons (a) and (b) all particles at Z = 41m

The left plot in Fig.6 shows the distribution of identified muons while the right one shows all particles. Note, that the area covers a zoom of the previous figure shifted up to cover the beam region. As is apparent from the right distribution there are extrapolated tracks in the whole region covered, whereas there is a hole in the muon distribution. The hole has a rectangular shape overlaid with a circular one. The rectangular hole is due to the beam hole in the second muon absorber MF2. Muons passing through this hole cannot be identified unless they pass through MF3 and H5I. These tracks are responsible for the high rate region left of the hole. The round hole overlaid with the rectangular one is most likely related to the beam hole of the MWPC chambers. The lower 5 cm of the rectangular hole is the region without muon tracks in the distribution of HM05 Fig.5. In this region there is no material for muon identification. Note, to avoid that this region gets larger in the future DVCS data taking due to the missing inner trigger, H5I and MF3 should be kept in the set-up for muon identification.

3. The rectangular region with a high number of extrapolations on the right side of the hole in fig.5 stems from the presence of GEM11 close to hodoscope improving the reconstruction considerably.

As the same features appear in the extrapolation and the tracks with hits the effects 1,2 and 3 are not visible in the efficiency histograms.

3.3 Efficiencies

The Efficiency $\eta = \frac{N_{hit}}{N_{pass}}$ equals the number of hits of muons divided by the number of passing muons. The number of hits, N_{hit}, equals the number of μ' extrapolations, which gave a hit in the geometrical acceptance of a plane; and the number of passing muons, N_{pass}, is the number of μ' extrapolations to the geometrical acceptance of a plane. The geometrical acceptance is checked by using the InActive function in PHAST. For the following plots the hodoscopes are divided in 6 bins per strip for ensuring a high resolution. The red colour indicates very high efficiency, whereas the blue colour shows a lesser efficiency. As an example, the centre of the outer hodoscope H4 with a high efficiency is shown in Fig. 7.The change between 2007 and 2010 are due to an elongation of the strips by 20 cm.

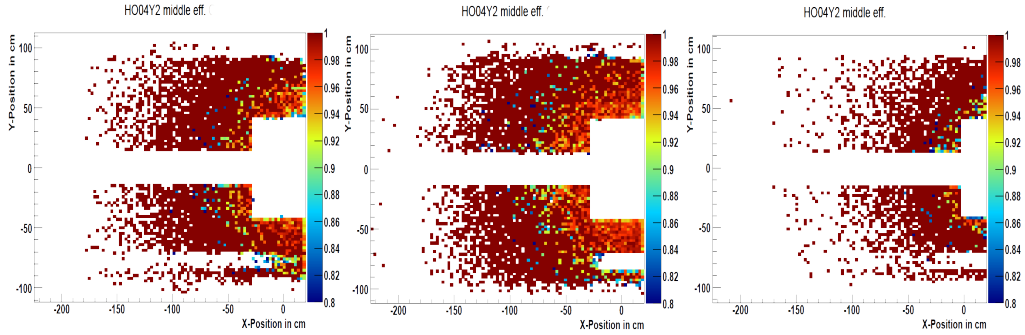

(a) 07W25 (b) 07W44 (c) 10W39

Figure 7: Efficiency of the hodosocope HO04

Summary

The hodoscope efficiencies are as high as before, but a more detailed investigation was needed. It turned out, that the horizontal bands in HL, HM occur because there are not many tracking planes measuring the corresponding coordinates. In the appendix the results for all hodoscope planes are shown. On the top rows the distribution of tracks within the hodoscope planes is shown, while in the lower picture the corresponding efficiency is shown.

The following problems are observed:

HM04X:	1-2 weak elements lower upper	 some insufficient overlaps some insufficient overlaps
HM04Y:	2 weak elements lower	 small region without muons
HM05X:	1-2 weak elements lower upper	 some insufficient overlaps some insufficient overlaps
HO03Y:	1-2 weak elements	 weak elements in bottom part
HO04Y2:	1-2 weak elements	 weak elements in bottom part
HI04X:	1-2 weak elements lower upper	 some insufficient overlaps some insufficient overlaps
HL05:		small region without muons

The authors thank Jens Barth, Yann Bedfer, Johannes Bernhard, Prometeusz Jasinski, Konrad Klimaszewski, Claude Marchand, Prof. Jörg Pretz and Malte Wilfert for helpful discussions.

List of Figures

References

[1] COMPASS, F. Gautheron et al., COMPASS II Proposal (2010) 84-88.

[2] COMPASS, P. Abbon et al., Nucl. Instrum. Meth. A 577 (2007) 491-494.

[3] COMPASS, C.Bernet et al., NIM A 550 (2005) 220-223.

[4] K.Klimaszweski, UserEvent42,
http : *//compass*02.*cern.ch/elog/High_pt/*42

4 Appendix

Appendix

List of Figures

Figure 1: Middle Trigger HM04X1 lower

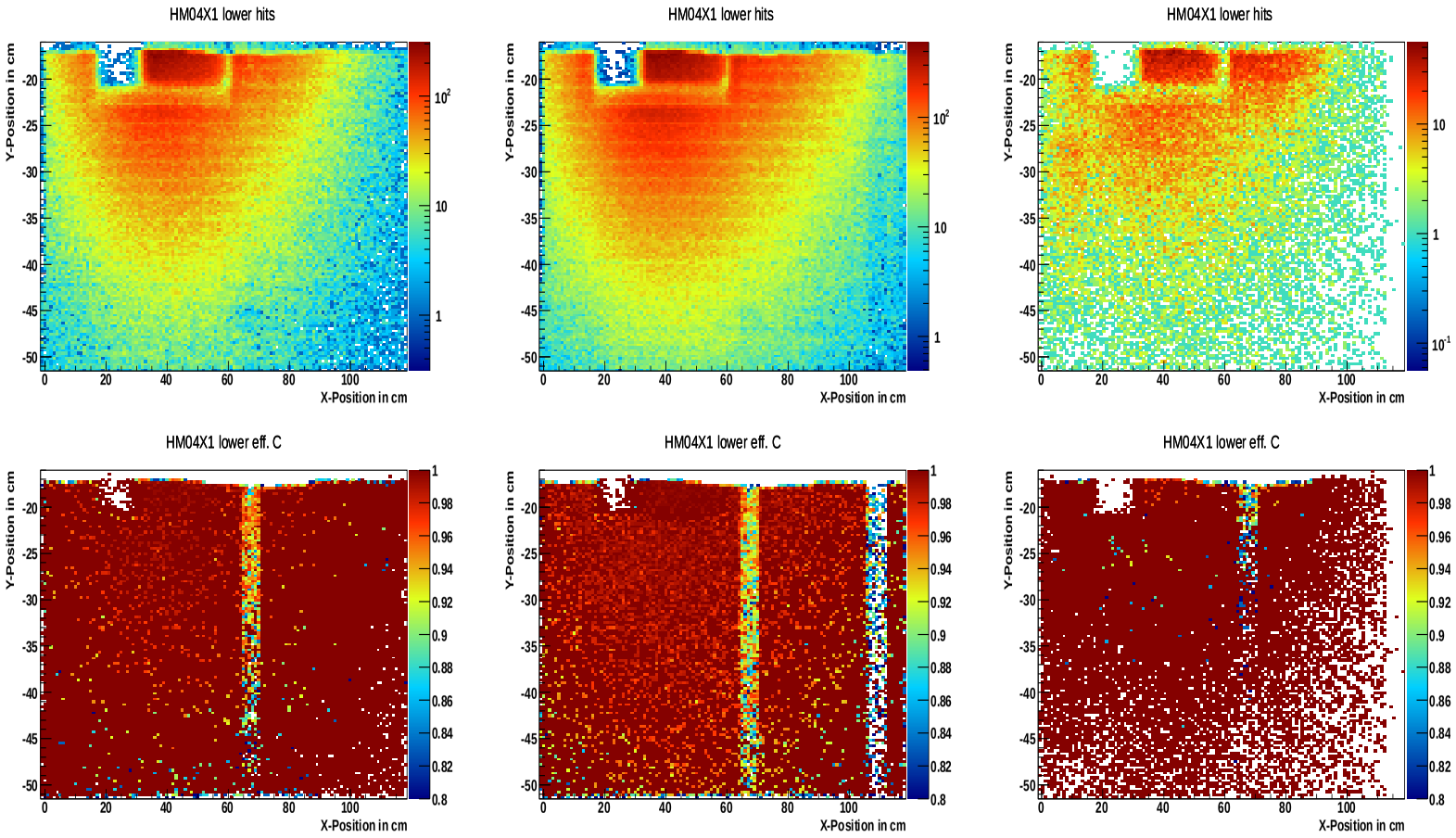

(a) W25 2007

(b) W44 2007

(c) W39 2010

Figure 2: Middle Trigger HM04X1 upper

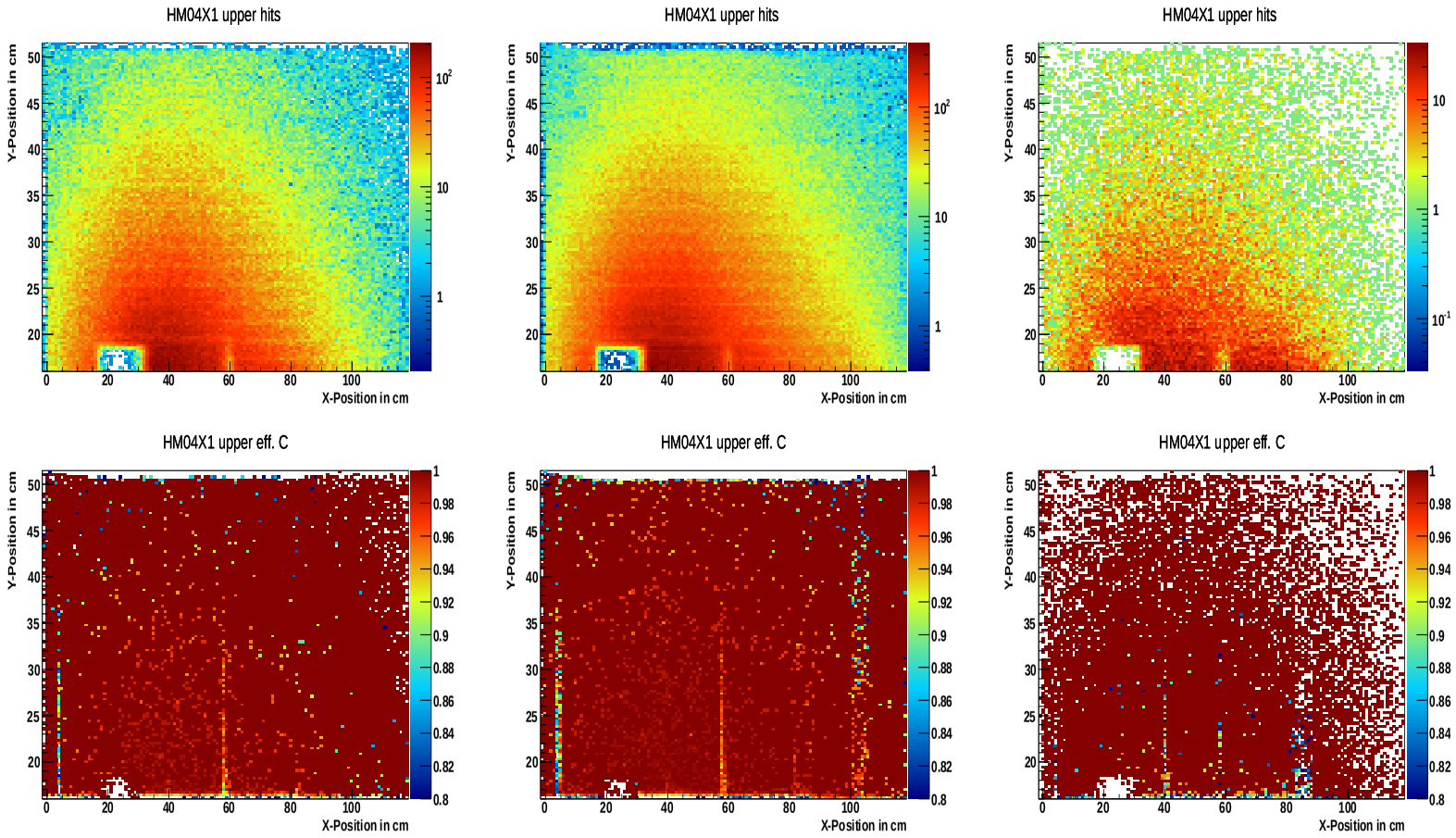

(a) W25 2007

(b) W44 2007

(c) W39 2010

Figure 3: Middle Trigger HM04Y1 lower

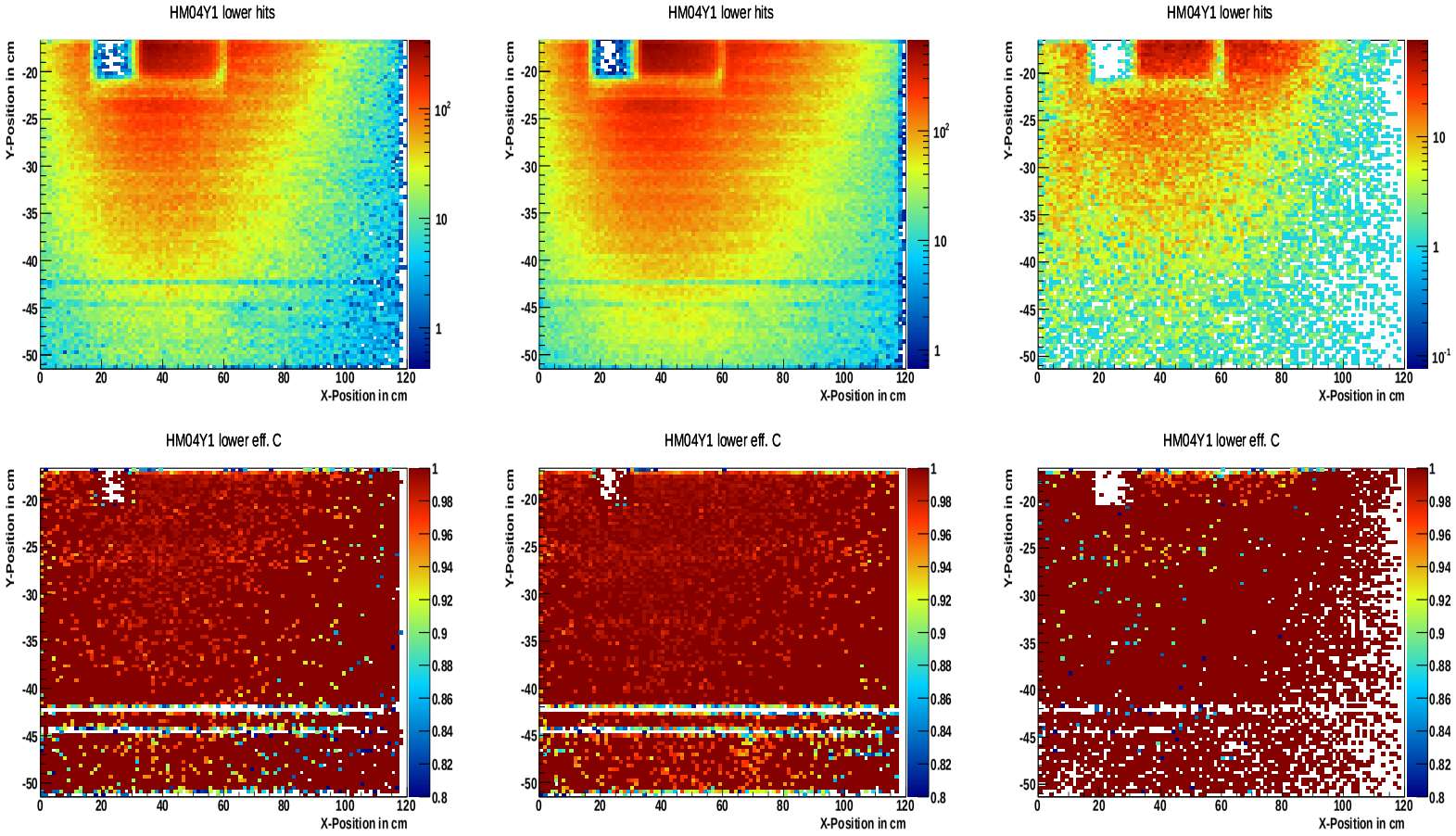

(a) W25 2007

(b) W44 2007

(c) W39 2010

Figure 4: Middle Trigger HM04Y1 upper

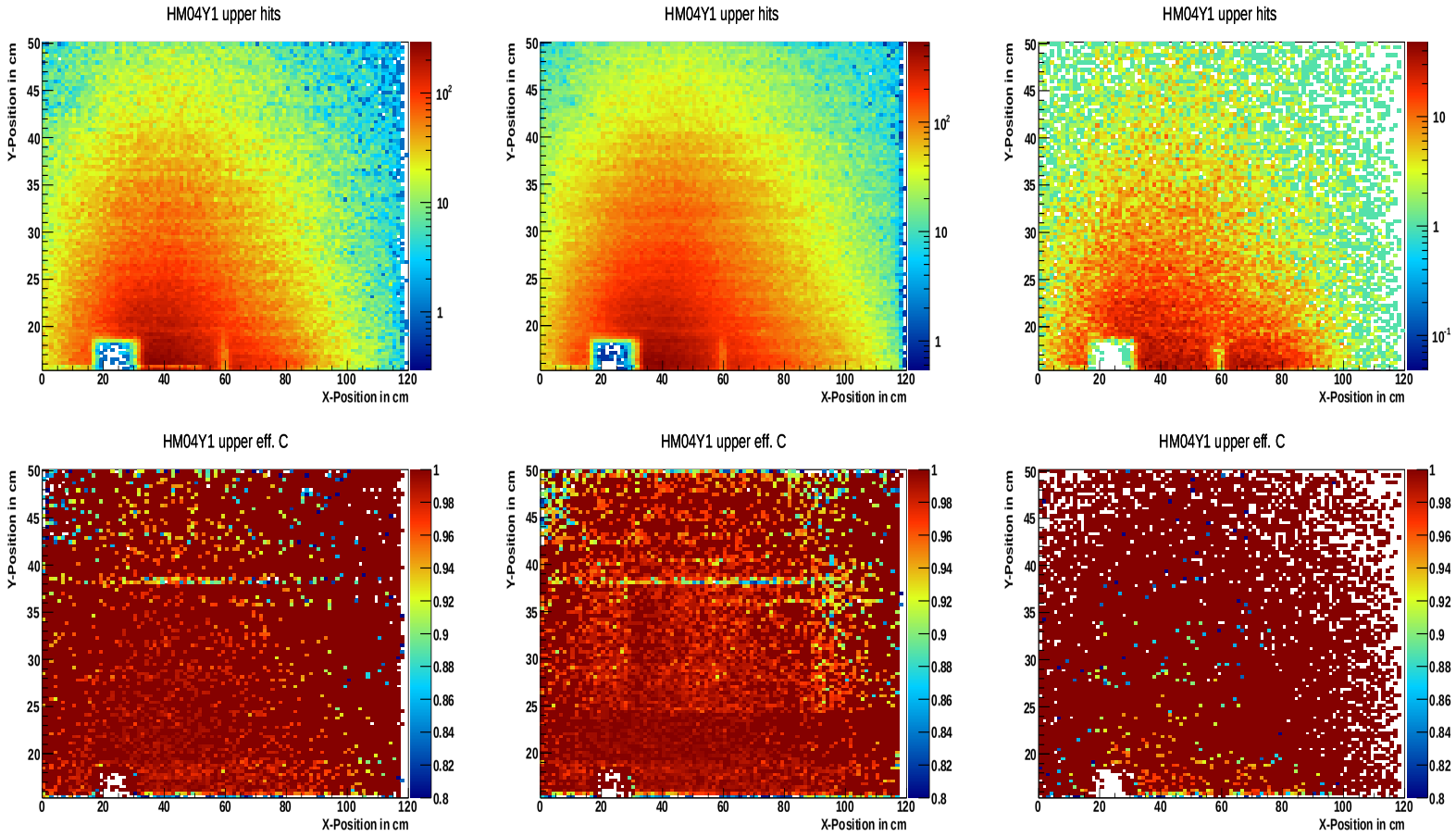

(a) W25 2007

(b) W44 2007

(c) W39 2010

Figure 5: Middle Trigger HM05X1 lower

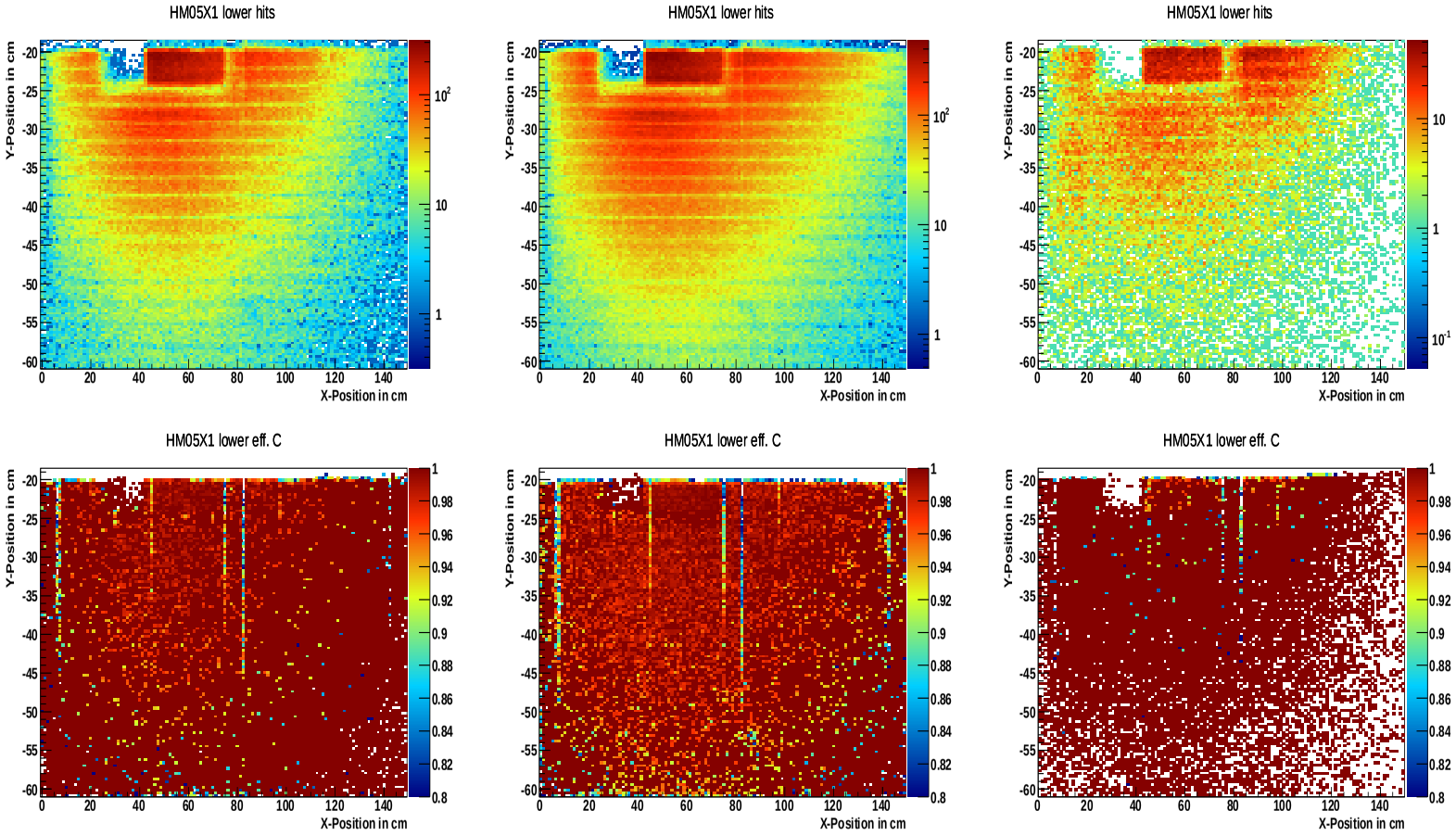

(a) W25 2007

(b) W44 2007

(c) W39 2010

Figure 6: Middle Trigger HM05X1 upper

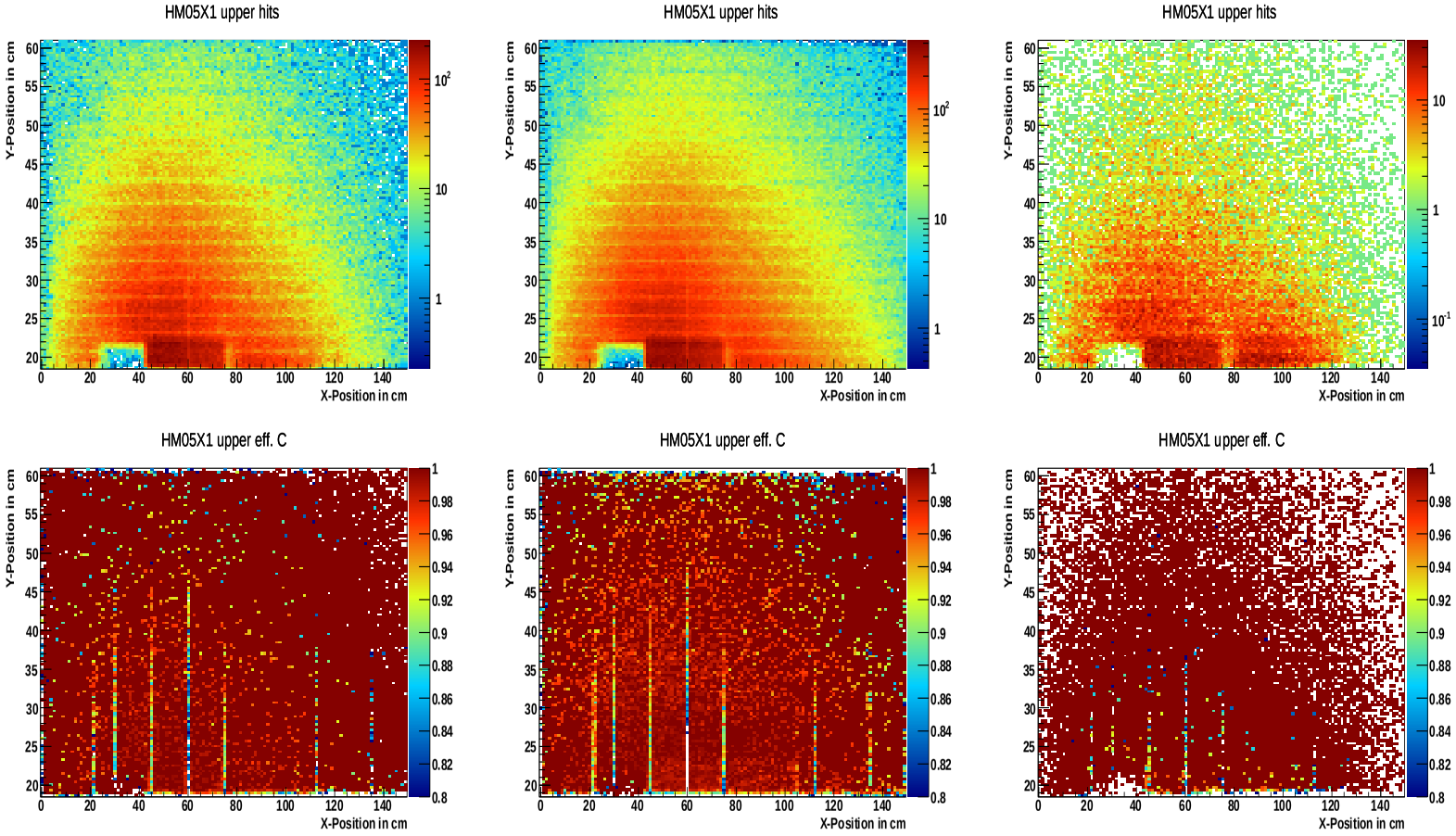

(a) W25 2007

(b) W44 2007

(c) W39 2010

Figure 7: Middle Trigger HM05Y1 lower

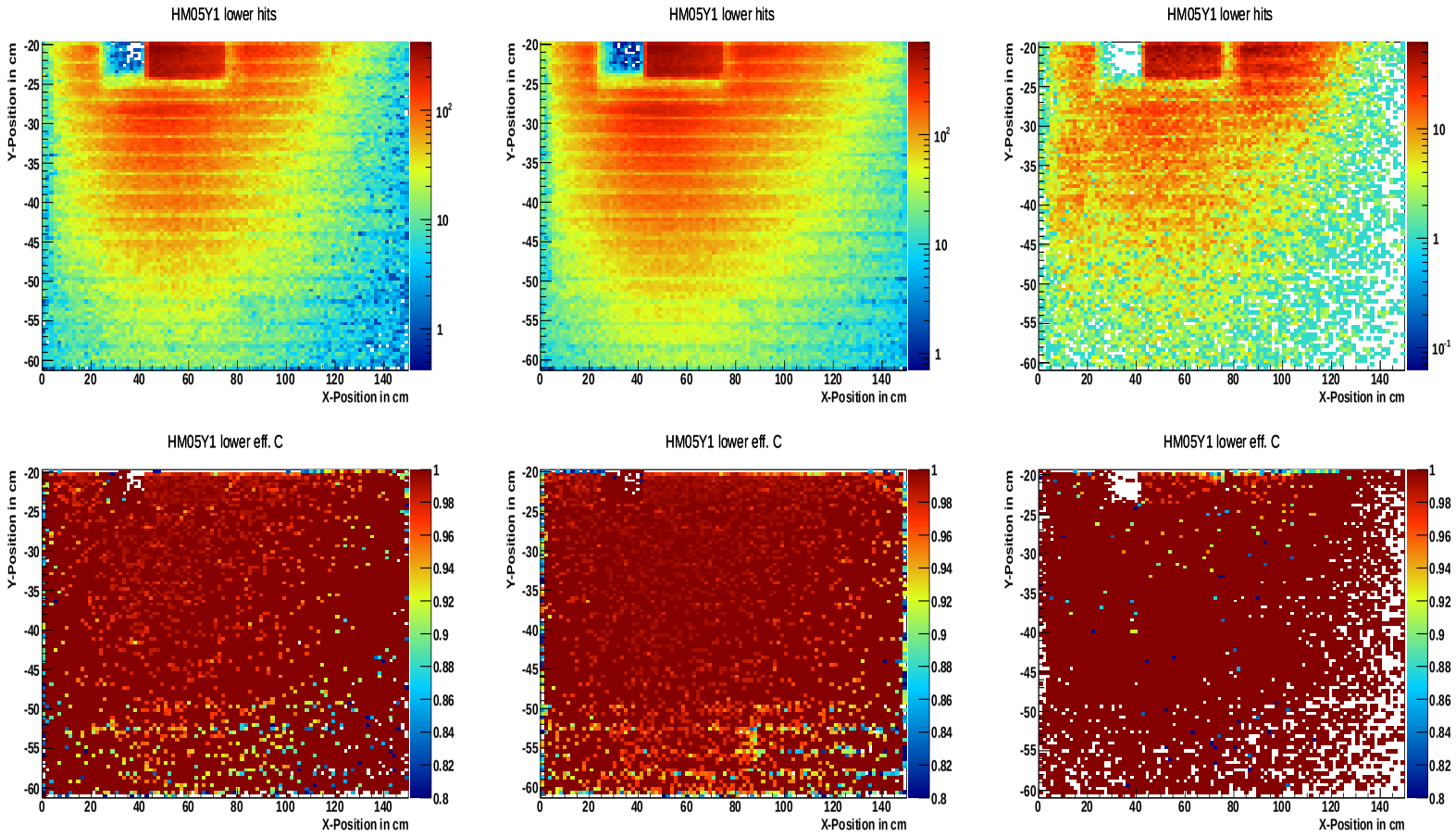

(a) W25 2007

(b) W44 2007

(c) W39 2010

Figure 8: Middle Trigger HM05Y1 upper

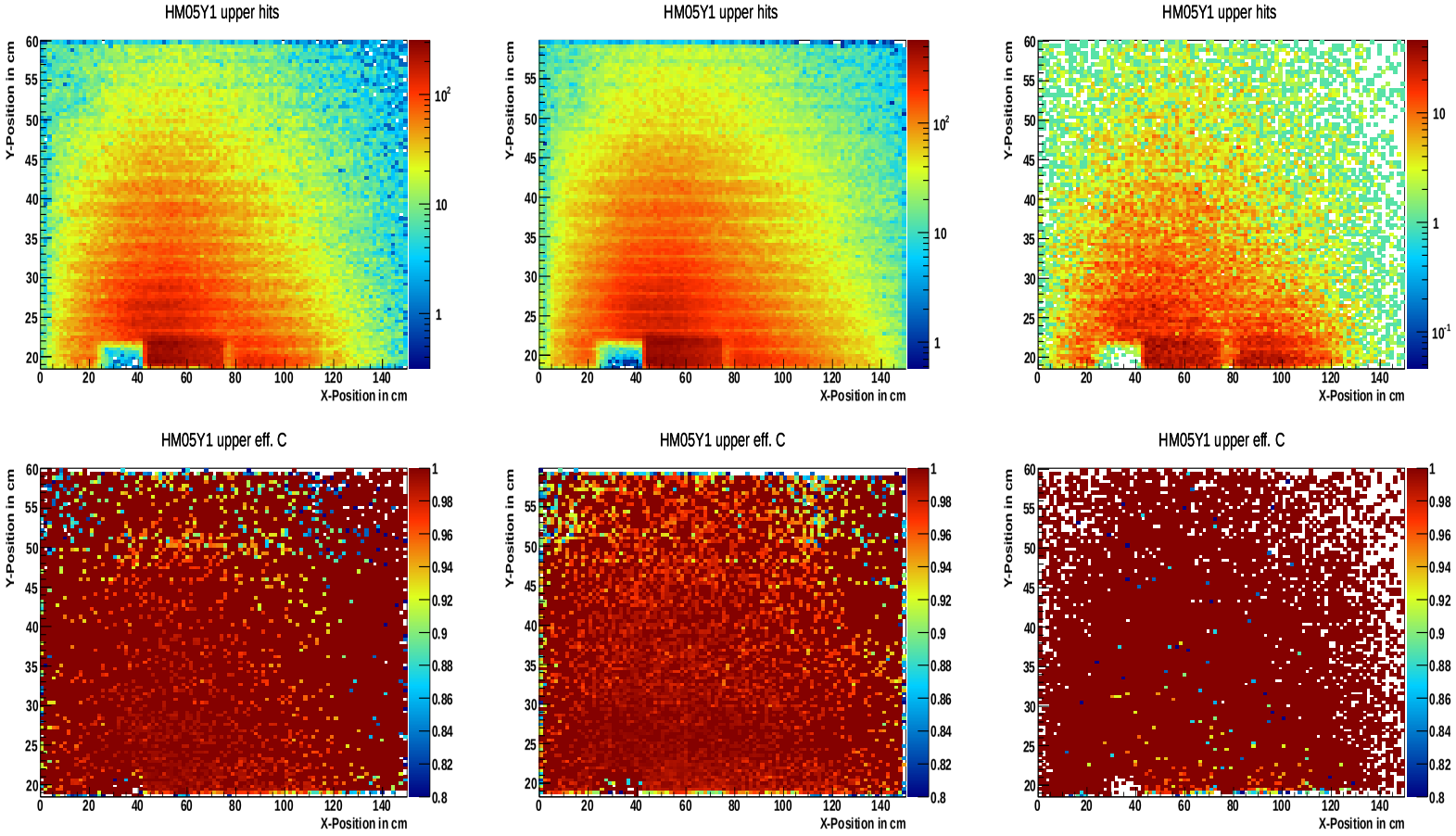

(a) W25 2007

(b) W44 2007

(c) W39 2010

Figure 9: Outer Trigger HO03

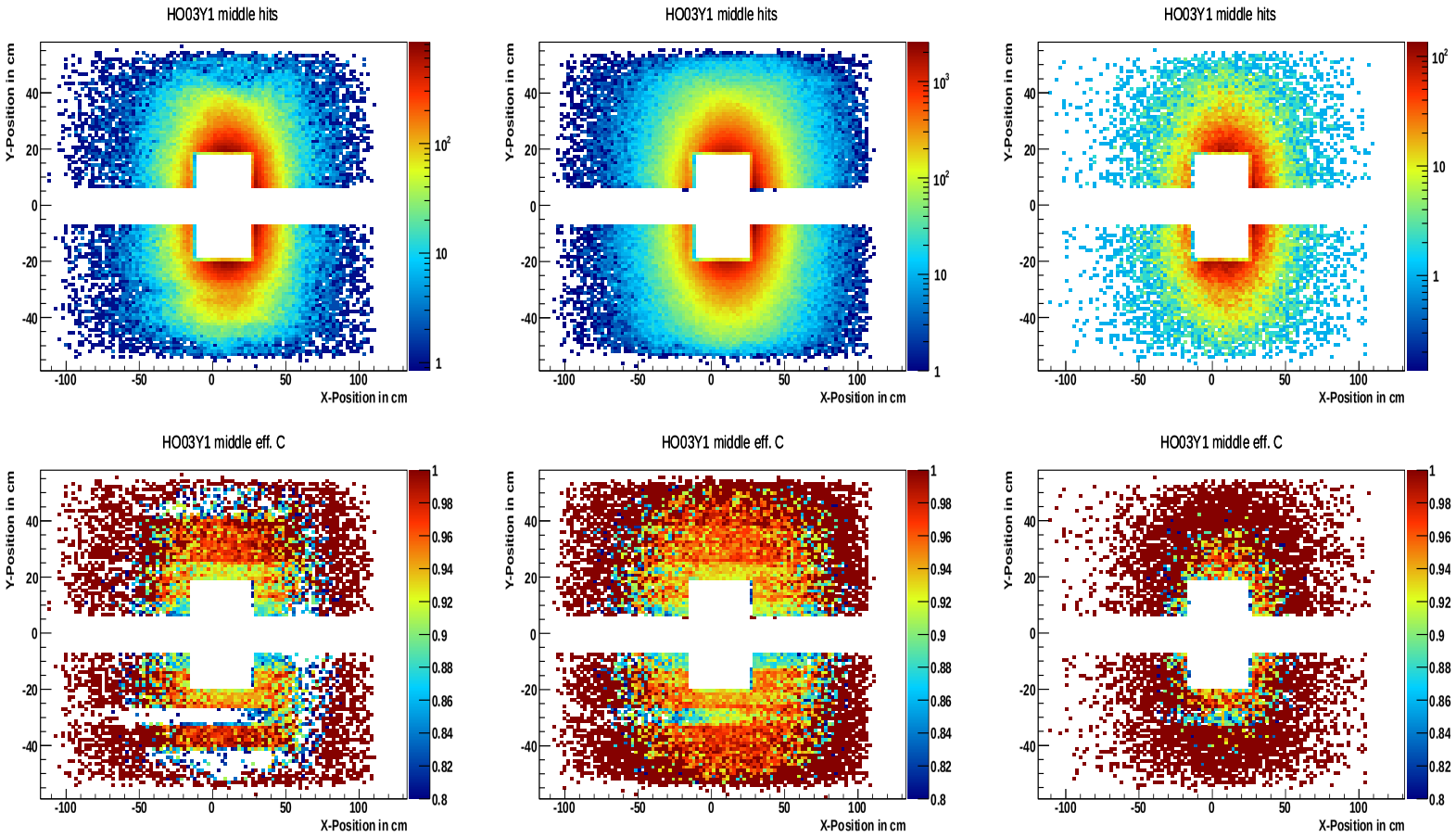

(a) W25 2007

(b) W44 2007

(c) W39 2010

Figure 10: Outer Trigger HO04Y1 - Jura

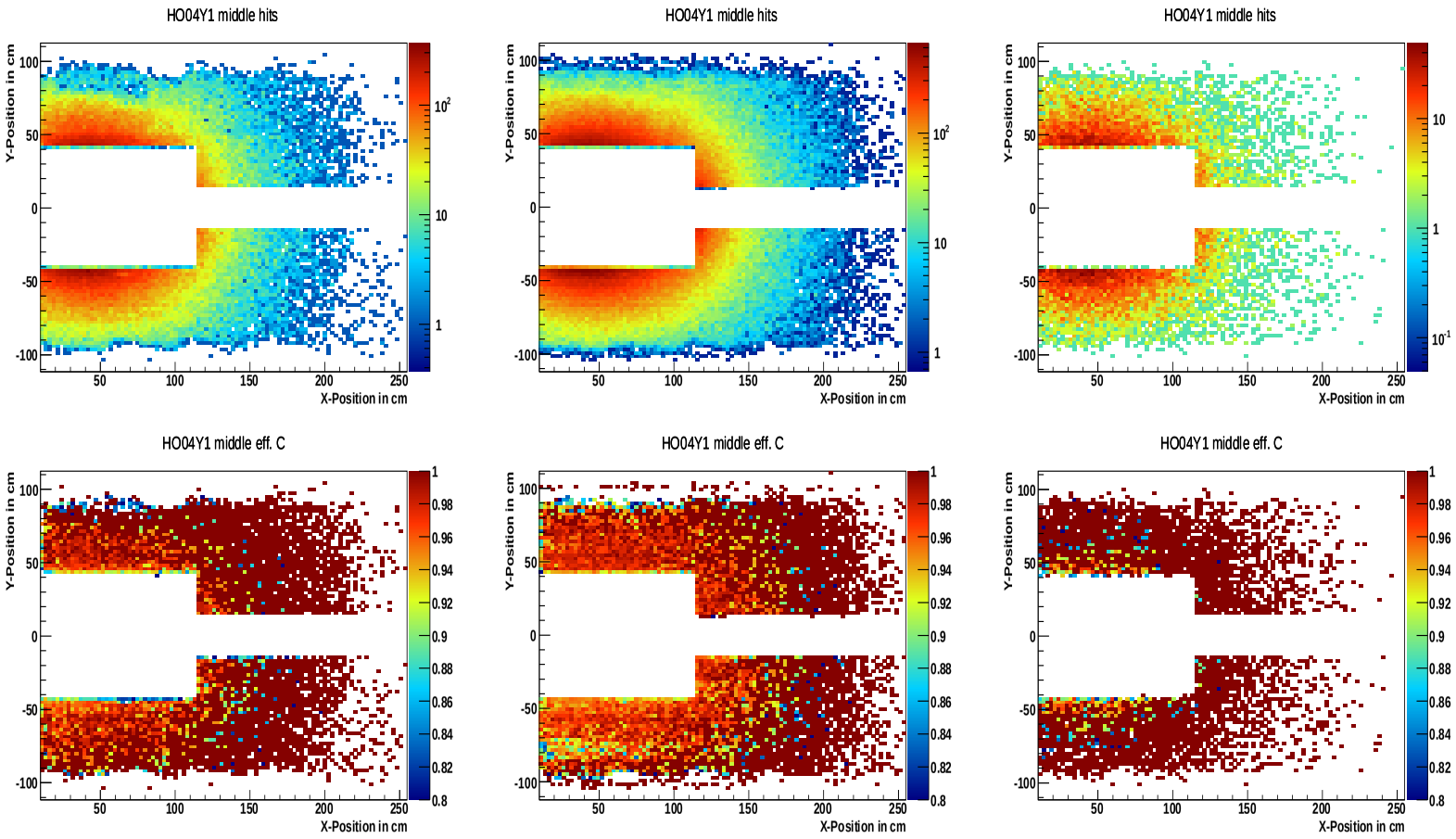

(a) W25 2007

(b) W44 2007

(c) W39 2010

Figure 11: Outer Trigger HO04Y2 - Salève

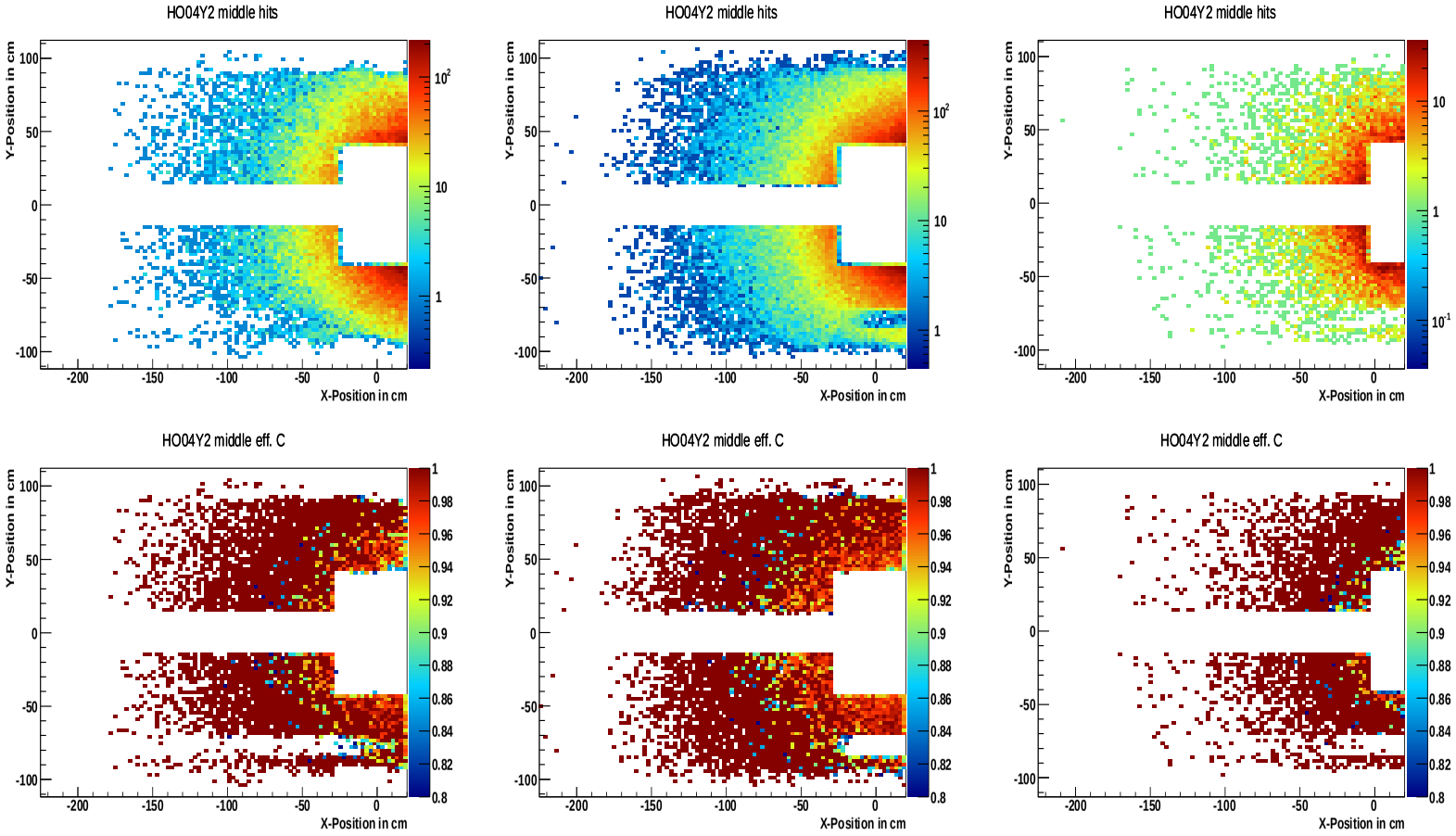

(a) W25 2007

(b) W44 2007

(c) W39 2010

Figure 12: Inner Trigger HI04X1 lower

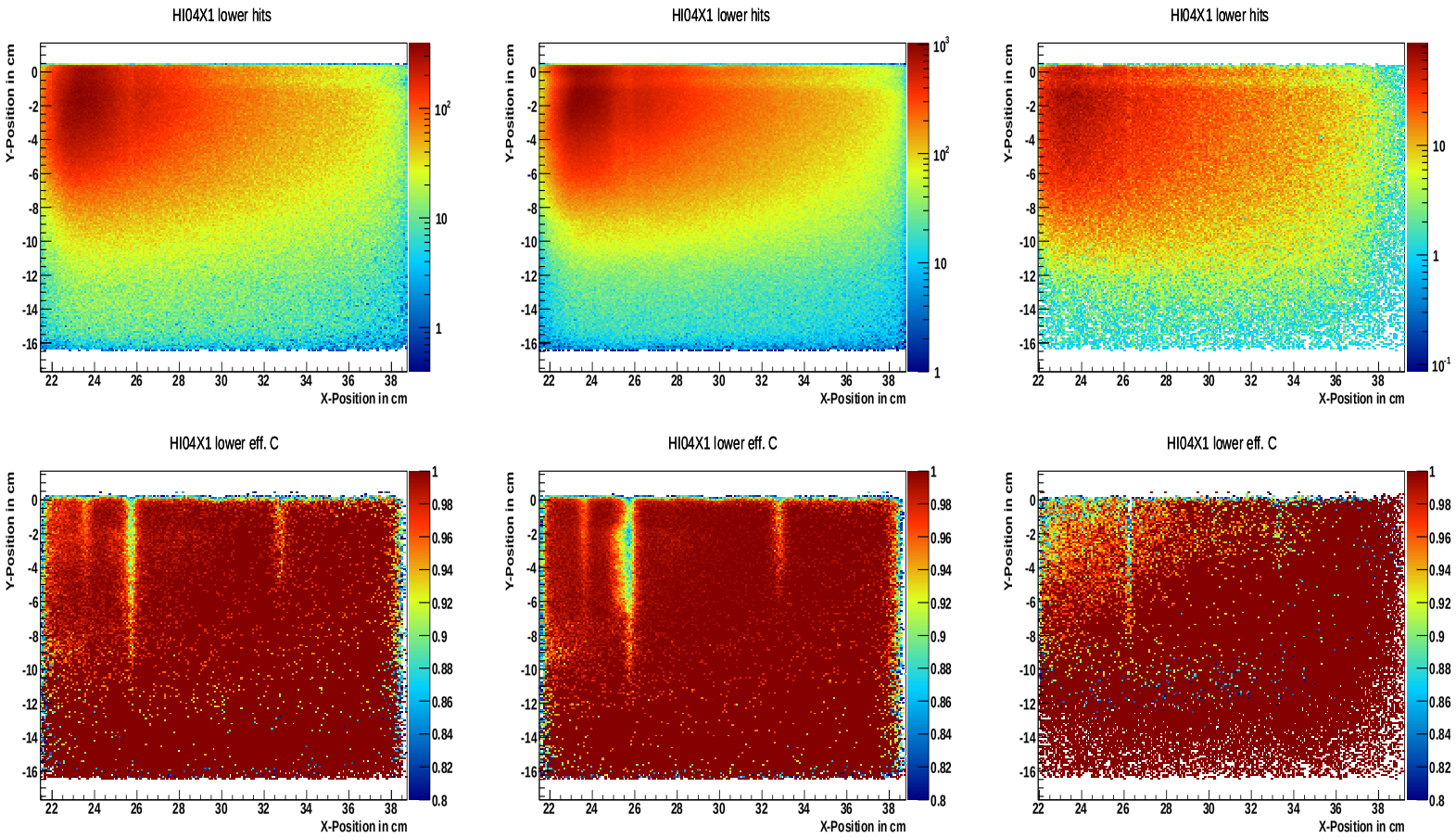

(a) W25 2007

(b) W44 2007

(c) W39 2010

Figure 13: Inner Trigger HI04X1 upper

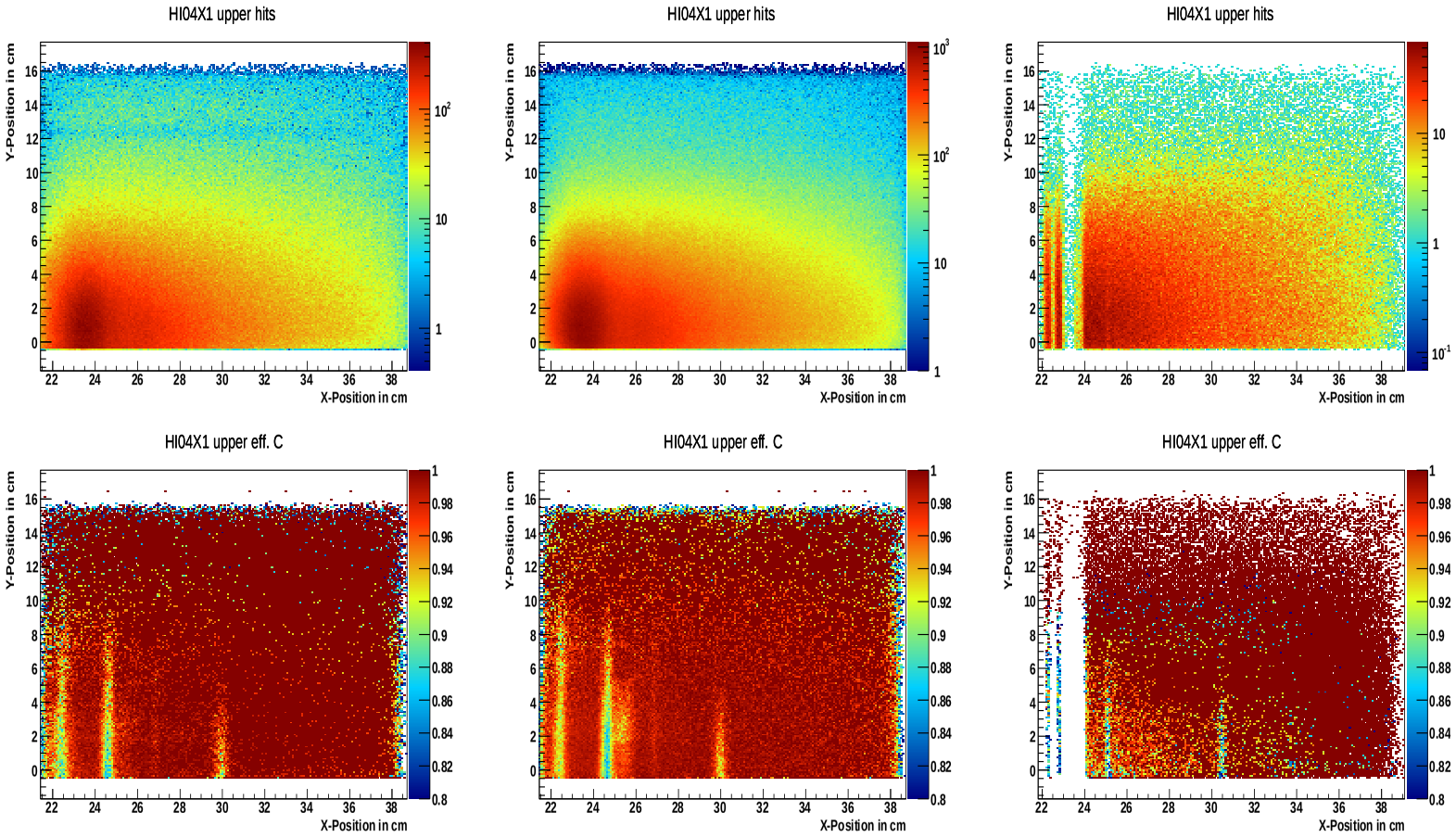

(a) W25 2007

(b) W44 2007

(c) W39 2010

Figure 14: Inner Trigger HI05X1 lower

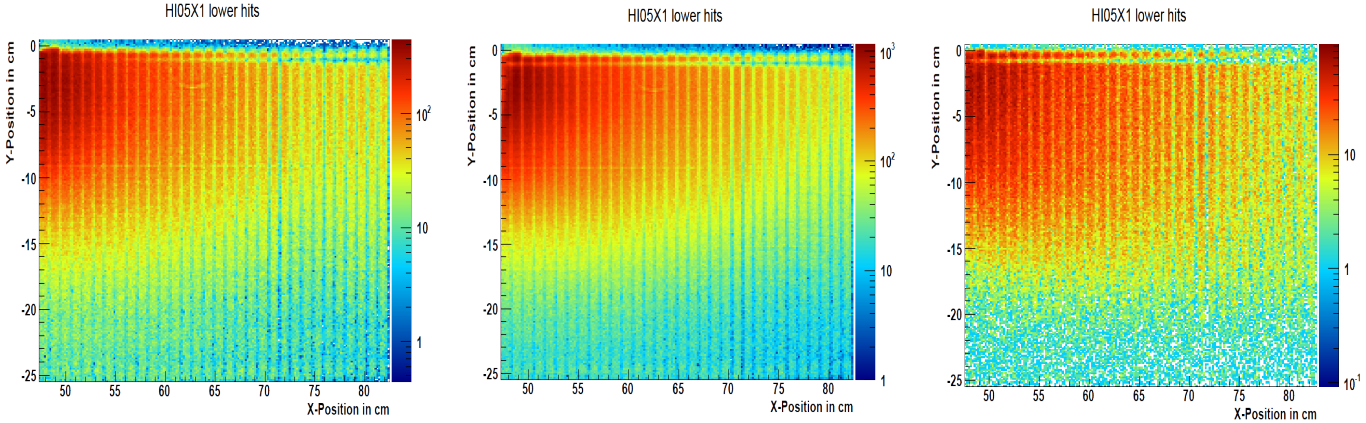

(a) W25 2007

(b) W44 2007

(c) W39 2010

Figure 15: Inner Trigger HI05X1 upper

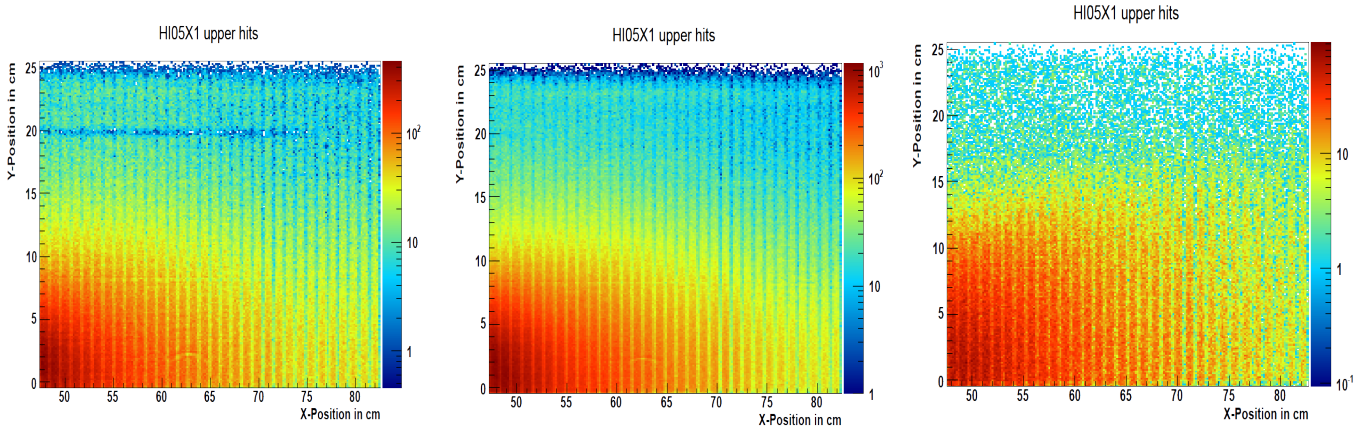

(a) W25 2007

(b) W44 2007

(c) W39 2010

ΔX

Figure 16: Ladder Trigger HL04X1

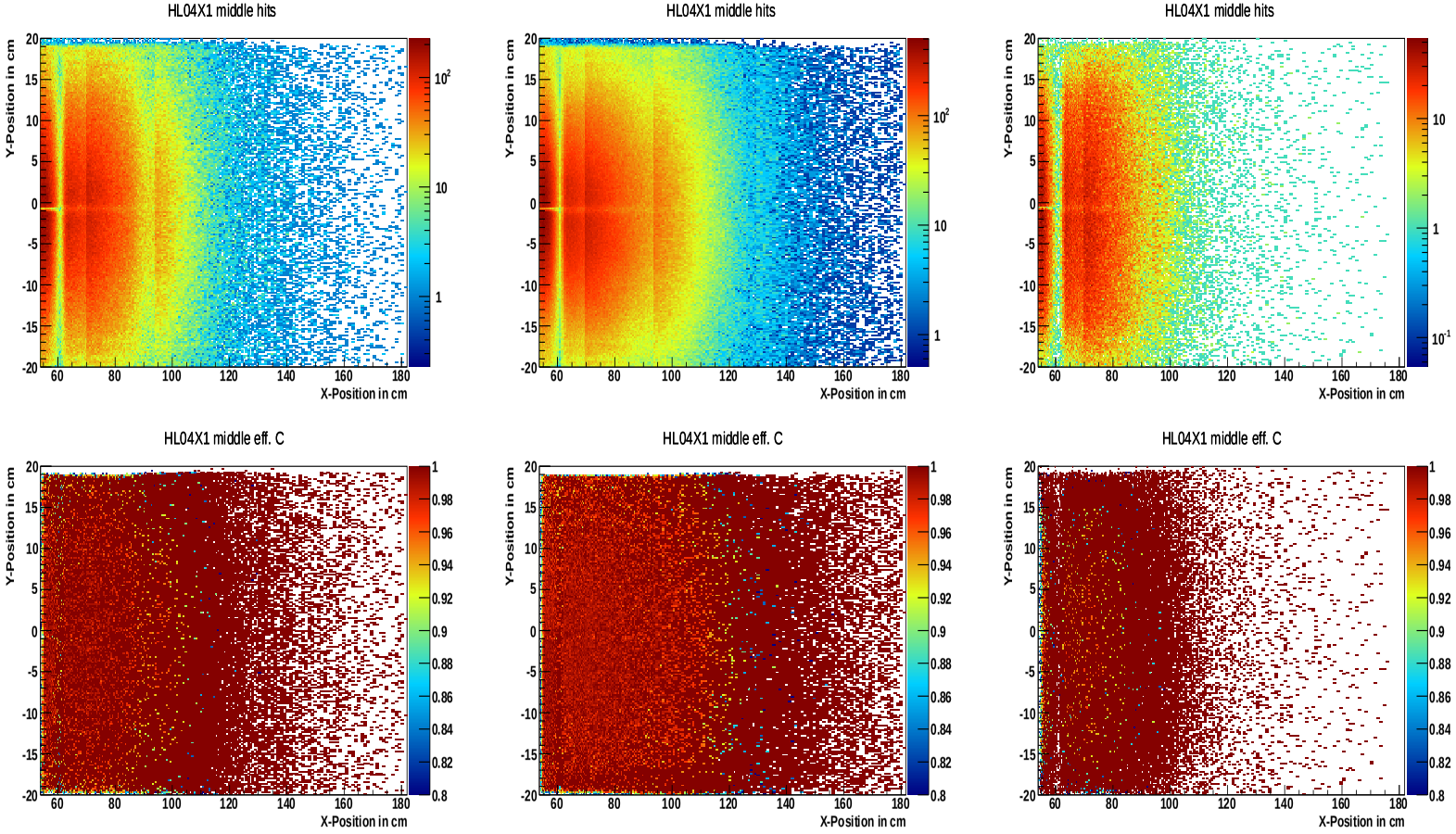

(a) W25 2007

(b) W44 2007

(c) W39 2010

Figure 17: Ladder Trigger HL05X1

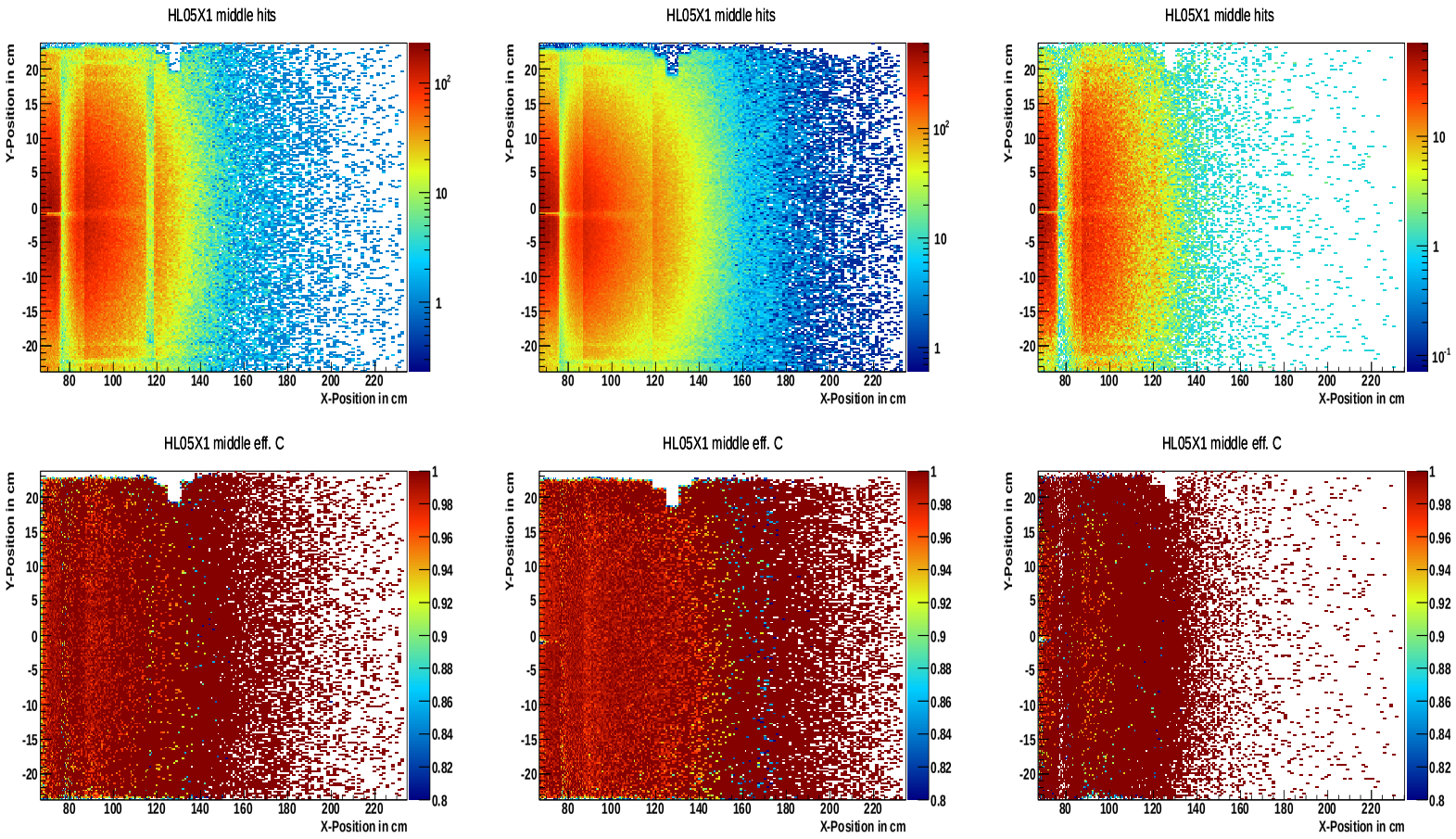

(a) W25 2007

(b) W44 2007

(c) W39 2010